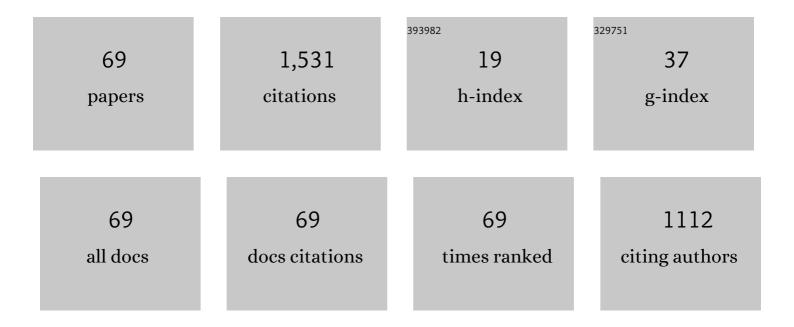
## Xingke Zhao

List of Publications by Year in descending order

Source: https://exaly.com/author-pdf/7480619/publications.pdf Version: 2024-02-01



#	Article	IF	CITATIONS
1	Reaction-composite diffusion brazing of C-SiC composite and Ni-based superalloy using mixed (Cu-Ti)+C powder as an interlayer. Journal of Materials Processing Technology, 2022, 300, 117419.	3.1	11
2	Microstructure and tribological behavior of the nickel-coated-graphite-reinforced Babbitt metal composite fabricated via selective laser melting. International Journal of Minerals, Metallurgy and Materials, 2022, 29, 320-326.	2.4	6
3	Study on the Kinetics of Ni3Sn4 Growth and Isothermal Solidification in Ni-Sn TLPS Bonding Process. Metallurgical and Materials Transactions A: Physical Metallurgy and Materials Science, 2022, 53, 1704-1716.	1.1	1
4	Study on microstructure evolution and reaction mechanism of in-flight Ti–Si–C agglomerates during reactive plasma spraying using in situ water quenching. Ceramics International, 2022, 48, 18866-18875.	2.3	3
5	Elastocaloric Performance of Pseudoelastic NiTi Coiled Wires. Shape Memory and Superelasticity, 2021, 7, 101-108.	1.1	4
6	Soldering Zr metallic glass to Ti alloy using pre-cladding ultrasonic processes. Welding in the World, Le Soudage Dans Le Monde, 2021, 65, 1225-1234.	1.3	4
7	Effect of Si content on the microstructure and properties of Ti–Si–C composite coatings prepared by reactive plasma spraying. Ceramics International, 2021, 47, 24438-24452.	2.3	10
8	Interfacial characteristics and mechanical properties of aluminum / steel butt joints fabricated by a newly developed high-frequency electric cooperated arc welding-brazing process. Journal of Materials Processing Technology, 2021, 298, 117317.	3.1	8
9	Transient Liquid-Phase Sintering Bonding Based on Cu40Sn60 (wt.%) Core/Shell Particles for High-Temperature Power Device Packaging. Journal of Electronic Materials, 2021, 50, 7283-7292.	1.0	6
10	Mechanisms of an innovative hybrid arc welding process in enhancing joint penetration and weld property control through resistive and induction heat. Journal of Manufacturing Processes, 2021, 72, 500-514.	2.8	5
11	Enhanced electrical conductivity and hardness of Copper/Carbon Nanotubes composite by tuning the interface structure. Materials Letters, 2020, 280, 128564.	1.3	18
12	Reactive composite-diffusing brazing of Cf/SiC composite and stainless steel with (Cu–15Ti)+C filler material. Materials Science & Engineering A: Structural Materials: Properties, Microstructure and Processing, 2020, 788, 139582.	2.6	14
13	In situ synthesis of TiC/Ti coatings by reactive plasma spraying. Materials Science and Technology, 2020, 36, 511-515.	0.8	4
14	Microstructure and properties of in-situ Ti5Si3-TiC composite coatings by reactive plasma spraying. Applied Surface Science, 2020, 508, 145264.	3.1	19
15	Join Al–steel dissimilar metal by novel high frequency electric cooperated arc welding. Science and Technology of Welding and Joining, 2019, 24, 721-723.	1.5	5
16	A novel process with the characteristics of low-temperature bonding and high-temperature resisting for joining Cf/SiC composite to GH3044 alloy. Journal of the European Ceramic Society, 2019, 39, 5468-5472.	2.8	12
17	Joining of high thermal-expansion mismatched C-SiC composite and stainless steel by an Ag + Ti + Mo mixed powder filler. Materials Letters, 2019, 256, 126632.	1.3	7
18	A Study on the Microstructures and Properties of Selective Laser Melted Babbitt Metals. Journal of Materials Engineering and Performance, 2019, 28, 5433-5440.	1.2	8

XINGKE ZHAO

#	Article	IF	CITATIONS
19	A novel high efficiency low heat input welding method: High frequency electric cooperated arc welding. Materials Letters, 2019, 252, 142-145.	1.3	5
20	Growth Kinetics of Ni3Sn4 in the Solid–Liquid Interfacial Reaction. Metallurgical and Materials Transactions A: Physical Metallurgy and Materials Science, 2019, 50, 3038-3043.	1.1	7
21	Effect of NiTi content and test temperature on mechanical behaviors of NiTi–PU composites. International Journal of Lightweight Materials and Manufacture, 2018, 1, 215-218.	1.3	2
22	Interfacial microstructure evolution and mechanical properties of TC4 alloy/304 stainless steel joints with different joining modes. Journal of Manufacturing Processes, 2018, 36, 115-125.	2.8	23
23	Microstructural Evolution of Ni-Sn Transient Liquid Phase Sintering Bond during High-Temperature Aging. Journal of Electronic Materials, 2018, 47, 4642-4652.	1.0	13
24	Evaluation on Dorsey Method in Surface Tension Measurement of Solder Liquids Containing Surfactants. International Journal of Thermophysics, 2018, 39, 1.	1.0	2
25	Mechanical activation of pre-alloyed NiTi2 and elemental Ni for the synthesis of NiTi alloys. Journal of Materials Science, 2018, 53, 13432-13441.	1.7	5
26	Joining of C f /SiC composite to Ti-6Al-4V with (Ti-Zr-Cu-Ni)+Ti filler based on in-situ alloying concept. Ceramics International, 2017, 43, 4151-4158.	2.3	23
27	Influence of Sr additions on microstructure and properties of Al–Si–Ge–Zn filler metal for brazing 6061 aluminum alloy. Journal of Materials Research, 2017, 32, 822-830.	1.2	4
28	Interfacial Behavior and Its Effect on Mechanical Properties of Cf/SiC Composite/TiAl6V4 Joint Brazed with TiZrCuNi. Journal of Materials Engineering and Performance, 2017, 26, 1114-1121.	1.2	6
29	Brazing of 6061 aluminum alloy with the novel Al-Si-Ge-Zn filler metal. Materials Letters, 2016, 179, 47-51.	1.3	15
30	Expanded Lever Rule for Phase Volume Fraction Calculation of High-Strength Low-Alloy Steel in Thermal Simulation. Metallurgical and Materials Transactions A: Physical Metallurgy and Materials Science, 2016, 47, 2795-2803.	1.1	7
31	Microstructures and Mechanical Properties of Laser Welding Joint of a CLAM Steel with Revised Chemical Compositions. Journal of Materials Engineering and Performance, 2016, 25, 1848-1855.	1.2	9
32	Correlation between microstructure and mechanical properties of active brazed Cf/SiC composite joints using Ti-Zr-Be. Materials Science & Engineering A: Structural Materials: Properties, Microstructure and Processing, 2016, 667, 332-339.	2.6	15
33	Interaction Between the Growth and Dissolution of Intermetallic Compounds in the Interfacial Reaction Between Solid Iron and Liquid Aluminum. Metallurgical and Materials Transactions A: Physical Metallurgy and Materials Science, 2016, 47, 5088-5100.	1.1	77
34	Laser penetration welding of an overlap titanium-on-aluminum configuration. International Journal of Advanced Manufacturing Technology, 2016, 87, 3069-3079.	1.5	29
35	Interface microstructure and fracture behavior of single/dual-beam laser welded steel-Al dissimilar joint produced with copper interlayer. International Journal of Advanced Manufacturing Technology, 2016, 82, 631-643.	1.5	71
36	A new partial transient liquid-phase bonding process with powder-mixture interlayer for bonding Cf/SiC composite and Ti–6Al–4V alloy. Materials Letters, 2015, 143, 237-240.	1.3	19

XINGKE ZHAO

#	Article	IF	CITATIONS
37	Preparation and Properties of a Novel Al-Si-Ge-Zn Filler Metal for Brazing Aluminum. Journal of Materials Engineering and Performance, 2015, 24, 2327-2334.	1.2	14
38	Influence of processing parameters on the characteristics of stainless steel/copper laser welding. Journal of Materials Processing Technology, 2015, 222, 43-51.	3.1	141
39	Microstructures and properties of double-ceramic-layer thermal barrier coatings of La2(Zr0.7Ce0.3)2O7/8YSZ made by atmospheric plasma spraying. Applied Surface Science, 2015, 340, 173-181.	3.1	46
40	An ultra-hard and thick composite coating metallurgically bonded to Ti–6Al–4V. Surface and Coatings Technology, 2015, 278, 157-162.	2.2	8
41	Characterization of Cu3P phase in Sn3.0Ag0.5Cu0.5P/Cu solder joints. International Journal of Minerals, Metallurgy and Materials, 2014, 21, 65-70.	2.4	1
42	Microstructures and Mechanical Properties of Laser Penetration Welding Joint With/Without Ni-Foil in an Overlap Steel-on-Aluminum Configuration. Metallurgical and Materials Transactions A: Physical Metallurgy and Materials Science, 2014, 45, 3064-3073.	1.1	50
43	Microstructures and mechanical property of laser butt welding of titanium alloy to stainless steel. Materials & Design, 2014, 53, 504-511.	5.1	171
44	Microstructures and mechanical properties of Cf/SiC composite and TC4 alloy joints brazed with (Ti–Zr–Cu–Ni)+W composite filler materials. Composites Science and Technology, 2014, 97, 19-26.	3.8	76
45	Active brazing of carbon fiber reinforced SiC composite and 304 stainless steel with Ti–Zr–Be. Materials Science & Engineering A: Structural Materials: Properties, Microstructure and Processing, 2014, 617, 66-72.	2.6	30
46	Microstructural Characteristics of a Stainless Steel/Copper Dissimilar Joint Made by Laser Welding. Metallurgical and Materials Transactions A: Physical Metallurgy and Materials Science, 2013, 44, 3690-3696.	1.1	103
47	Phase structure and thermophysical properties of co-doped La2Zr2O7 ceramics for thermal barrier coatings. Ceramics International, 2012, 38, 3607-3612.	2.3	63
48	Influence of a Ni-foil interlayer on Fe/Al dissimilar joint by laser penetration welding. Materials Letters, 2012, 79, 296-299.	1.3	75
49	Superplastic deformation mechanism and mechanical behavior of a laser-welded Ti–6Al–4V alloy joint. Materials Science & Engineering A: Structural Materials: Properties, Microstructure and Processing, 2012, 541, 110-119.	2.6	36
50	THERMAL SHOCK RESISTANCE OF La2(Zr0.7Ce0.3)2O7 THERMAL BARRIER COATING PREPARED BY ATMOSPHERIC PLASMA SPRAYING. Jinshu Xuebao/Acta Metallurgica Sinica, 2012, 48, 965.	0.3	1
51	Martensitic transformation behaviour of non-equilibrium heat treated Ni50·9Ti49·1 alloys. Materials Science and Technology, 2011, 27, 437-439.	0.8	1
52	Growth Behavior of Intermetallic Compounds at SnAgCu/Ni and Cu Interfaces. Journal of Materials Engineering and Performance, 2010, 19, 129-134.	1.2	10
53	Mechanical properties of additive laser-welded NiTi alloy. Materials Letters, 2010, 64, 628-631.	1.3	14
54	Microstructure and superplasticity of laser welded Ti–6Al–4V alloy. Materials & Design, 2010, 31, 620-623.	5.1	13

XINGKE ZHAO

#	ARTICLE	IF	CITATIONS
55	Pore structures of high-porosity NiTi alloys made from elemental powders with NaCl temporary space-holders. Materials Letters, 2009, 63, 2402-2404.	1.3	40
56	Vacuum brazing of NiTi alloy by AgCu eutectic filler. Materials Science and Technology, 2009, 25, 1495-1497.	0.8	8
57	Effect of thermal-shearing cycling on Ag3Sn microstructural coarsening in SnAgCu solder. Journal of Alloys and Compounds, 2009, 469, 102-107.	2.8	34
58	Microstructure and properties of TiC–Fe36Ni cermet coatings by reactive plasma spraying using sucrose as carbonaceous precursor. Applied Surface Science, 2008, 254, 6687-6692.	3.1	13
59	Microstructures of cerium added laser weld of a TiNi alloy. Materials Letters, 2008, 62, 1551-1553.	1.3	22
60	In-situ synthesis and microstructure of TiC–Fe36Ni composite coatings by reactive detonation-gun spraying. Materials Letters, 2008, 62, 2009-2012.	1.3	11
61	Two-stage superelasticity of a Ce-added laser-welded TiNi alloy. Materials Letters, 2008, 62, 3539-3541.	1.3	10
62	Microstructural Transformation on SnAgCu/Cu Interface Induced by Thermal-shearing Cycling. , 2008, , .		0
63	Effect of Thermal-Shearing Induced Microstructural Coarsening on SnAgCu Microelectronic Solder. , 2007, , .		0
64	TLP bonding of SiCp/2618Al composites using mixed Al–Ag–Cu system powders as interlayers. Journal of Materials Science, 2007, 42, 9746-9749.	1.7	7
65	Growth Behavior of IMCs and Fracture Forming Mechanism at Sn-Ag-Cu/Cu Interfaces under Thermal-Shearing Cycling Condition. , 2006, , .		1
66	Joints of Cf/SiC Composite to Ti-Alloy with <i>In-Situ</i> Synthesized TiC <i><sub>x</sub></i> Improved Brazing Layers. Materials Transactions, 2006, 47, 1261-1263.	0.4	15
67	Morphology and hydrophobicity of a polyurethane film molded on a porous anodic alumina template. Surface and Coatings Technology, 2006, 200, 3492-3495.	2.2	17
68	Microstructure of phosphorus ion-implanted TiNi alloy. Journal of Materials Science, 2005, 40, 5291-5293.	1.7	0
69	Corrosion behavior of phosphorus ion-implanted Ni50.6Ti49.4 shape memory alloy. Surface and Coatings Technology, 2002, 155, 236-238.	2.2	23